Glycoconjugate Journal 16, 257–264 (1999)

Structural definition of arabinomannans from *Mycobacterium bovis* BCG

*Jérôme Nigou, Martine Gilleron, Thérèse Brando, Alain Vercellone and Germain Puzo**

Institut de Pharmacologie et de Biologie Structurale du Centre National de la Recherche Scientifique, UPR 9062, 205 route de Narbonne, 31077 Toulouse Cedex, France

The structures of the hydrophilic parietal and cellular arabinomannans isolated from *Mycobacterium bovis* BCG cell wall [Nigou *et al.* (1997) *J Biol Chem* 272: 23094–103] were investigated. Their molecular mass as determined by MALDI-TOF mass spectrometry was around 16 kDa. Concerning cap structure, capillary electrophoresis analysis demonstrated that dimannoside (Man*p*α1→2Man*p*) was the most abundant motif (65–75%). Using two-dimensional ^{1}H-^{13}C NMR spectroscopy, the mannan core was unambiguously demonstrated to be composed of →6Man*p*α1→ backbone substituted at some O-2 by a single Man*p* unit. The branching degree was determined as 84%. Finally, arabinomannans were found to be devoid of the phosphatidyl-*myo*-inositol anchor and, by aminonaphthalene disulfonate tagging, the mannan core was shown to contain a reducing end. This constitutes the main difference between arabinomannans and lipoarabinomannans from *Mycobacterium bovis* BCG.

Keywords: **mycobacteria, BCG, polysaccharide, arabinomannan, structure.**

Abbreviations: **AMs: arabinomannans; ANDS: aminonaphthalene disulfonate; APTS: 1-aminopyrene-3,6,8-trisulfonate; Ara*f*: arabinofuranose; BCG: Bacille de Calmette et Guérin; cAMs, cManAMs: cellular AMs, cellular ManAMs; CZE: capillary electrophoresis; HMBC: heteronuclear multiple bond correlation; HMQC: heteronuclear multiple quantum correlation; LAMs: lipoarabinomannans; HOHAHA: homonuclear Hartman Hahn correlation; LMs: lipomannans; MALDI-TOF: Matrix-assisted laser desorption-ionization - time of flight; ManAMs: mannose-capped arabinomannans; ManLAMs: mannose-capped lipoarabinomannans; Man*p*: mannopyranose; pAMs, pManAMs: parietal AMs, parietal ManAMs; PI anchor: phosphatidyl-*myo*-inositol anchor; 1D: one-dimensional; 2D: two-dimensional; 6-α-Man*p* represents→6Man*p*α1→.**

Introduction

Mycobacteria are the causative agents of tuberculosis and leprosy [1]. Among the glycoconjugates in the mycobacterial cell envelope, lipoarabinomannans (LAMs) are of particular interest as they are pivotal antigens of mycobacteria (for reviews, see [2,3]). Indeed, LAMs modulate cytokine secretion from immune cells, such as macrophages [4–7], polymorphonuclear granulocytes [8] or human dendritic cells [9]. Moreover, mannose-capped LAMs (ManLAMs) from *Mycobacterium tuberculosis* [10] and *Mycobacterium bovis* BCG [11] bind murine and human macrophages via the mannose receptor. Finally, ManLAMs from *Mycobacterium leprae* and *M. tuberculosis* are presented by CD1 molecules and stimulate CD4/CD8 double negative *αβ*T cells [12].

Structurally, ManLAMs, isolated from *M. tuberculosis, M. leprae* and *M. bovis* BCG, are composed of four domains, a phosphatidyl-*myo*-inositol anchor (PI anchor), a mannan core, an arabinan domain and mannooligosaccharide caps. Despite different biological activities of ManLAMs of different mycobacterial origins, to date, all the ManLAMs investigated have a similar basic structure.

Recently, we reported a new method for extracting ManLAMs from *M. bovis* BCG, enabling isolation of parietal and cellular ManLAMs [13]. The relevance of this separation was supported by the obtaining of ManLAMs differing in their capping degree and in anchor structure [9,14] and which stimulated TNF-α and IL-8 secretion from human dendritic cells to different extents [9]. In addition, the use of a Triton X-114 phase separation method permitted separation of amphipathic lipoglycans, ManLAMs and lipomannans (LMs) from the hydrophilic polysaccharides structurally related to ManLAMs, arabinomannans (AMs). Interestingly, AMs exhibited quite different biological properties to those of the ManLAMs. For example, they did not induce TNF-α and IL-8 release by human dendritic cells [9].

We report here the structural characterization of parietal

*To whom correspondence should be addressed. Tel: 33 5 61 17 55 04; Fax: 33 5 61 17 55 05; E-mail: *germain@ipbs.fr*

and cellular AMs (pAMs and cAMs, respectively) from *M. bovis* BCG. Study of these molecules structurally related to ManLAMs should help establish a structural basis for the biological activities of LAMs.

Materials and methods

ManAMs extraction and purification

pAMs and cAMs were purified as previously described [9]. Briefly, *M. bovis* BCG Pasteur strain cells were delipidated using $CHCl_3/CH_3OH$, 1:1, v/v. The delipidated mycobacteria were extracted six times by refluxing in 50% ethanol at 65 °C for 8 h (parietal fraction). The resulting cells (cellular fraction) were washed and disintegrated using a French pressure cell (one step of lysis at a pressure maintained above 200 MPa) and in ice by sonication (20 kHz, 600 W, 15 min). Most of the proteins of the cellular fraction were removed by a hot 80% (w/w) aqueous phenol biphasic wash at 70 °C for 1 h. After enzymatic treatments with trypsin, α-amylase, RNase A (from bovine pancreas, Sigma, Saint-Quentin Fallavier, France) and DNase I (from bovine pancreas, Fluka, Saint-Quentin Fallavier, France), dialysis removed the aminoacids, glucose and nucleotides from the glycans and lipoglycans of parietal and cellular fractions. A Triton X-114 phase separation technique was applied to glycan and lipoglycan mixtures. AMs, recovered in the detergent-depleted phase, were finally purified by gel filtration. The sample was dissolved in 0.2 M NaCl, 0.25% sodium deoxycholate (w/v), 1 mM ethylenediaminetetraacetic acid disodium salt and 10 mM Tris pH 8 to a final concentration of 200 mg/ml, incubated two days at room temperature and loaded on a Bio-Gel P-100 column (52 × 3 cm) eluted with the same buffer at a flow rate of 5 ml/h.

Matrix-assisted laser desorption-ionization mass spectrometry (MALDI/MS)

AM samples were prepared as previously described [15]. The matrix used was super-DHB, a 9:1 mixture of 2,5-dihydroxybenzoic acid with 2-hydroxy-5-methoxybenzoic acid [16]. Analyses were performed on a Dynamo 1.2 m linear MALDI-time-of-flight (TOF) mass spectrometer. External calibration was used with dynamic ion extraction.

ManAM labelling and electrophoresis [17]

Each dry sample was mixed with 1 µl of 0.2 M aminonaphthalene disulfonate (ANDS) in 15 % acetic acid and 1 µl of 1 M sodium cyanoborohydride in tetrahydrofuran (Aldrich). The reaction was performed for 90 min at 55 °C [18]. The reaction mixture was loaded into wells of polyacrylamide gels (8 × 9 cm) [19]. The separating gel was composed of 15% acrylamide (19:1 ratio of acrylamide to N,N′-methylene-bisacrylamide as cross-linker). A 5% acrylamide gel was layered above the separating gel. Samples were electrophoresed first at 20 V and finally at 150 V. Gels were photographed after removal from their cassettes and placing on a UV light box with a maximum emission wavelength of 254 nm.

Capillary electrophoresis of mild acidic hydrolyzed AMs (0.1 M HCl at 110 °C for 30 min) was performed as previously described for ManLAMs [9]. Acetic acid 1% (w/v), triethylamine 30mM in water, pH 3.5 was used as running electrolyte. 1-aminopyrene-3,6,8-trisulfonate (APTS) was purchased from Interchim, Montluçon, France.

NMR Spectroscopy

NMR spectra were recorded on a Bruker DMX-500 spectrometer equipped with an Aspect X32 computer. Samples (60 mg ManLAMs, 20 mg native AMs, 2.5 mg mannan core) were exchanged in D_2O (D, 99.97% from Euriso-top, Saint-Aubin, France), with intermediate lyophilization, then dissolved in 0.4 ml D_2O and analyzed in 200 × 5 mm 535-PP NMR tubes. Spectra were recorded at 313 K.

The one dimensional (1D) proton (^1H) spectra were measured using a 90° tipping angle for the pulse and 1 s as recycle delay between each of the 8 (for native AMs and ManLAMs) and 256 (for mannan core) acquisitions of 1.64 s. The spectral width (SW) of 4505 Hz was collected in 16 k complex points that were multiplied by a Gaussian function (LB = −1, GB = 0.2) prior to processing to 32 k real points in the frequency domain. After Fourier transformation, the spectra were base-line corrected with a fourth order polynomial function. The ^1H NMR chemical shifts were referenced relative to internal acetone at 2.225 ppm. All two-dimensional (2D) spectra were recorded without sample spinning and data were acquired in the phase sensitive mode using the time-proportional phase increment (TPPI) method [20].

The 2D ^1H-^{13}C Heteronuclear Multiple Quantum Correlation (HMQC), ^1H-^{13}C HMQC-Homonuclear Hartman Hahn correlation (HOHAHA) and ^1H-^{13}C Heteronuclear Multiple Bond Correlation (HMBC) spectra were recorded in the proton-detected mode with a Bruker 5-mm ^1H broad band tunable probe with reverse geometry. The Globally optimized Alterning-phase Rectangular Pulses (GARP) sequence [21] at the carbon frequency was used as a composite pulse decoupling during acquisition. The single-bond HMQC spectrum was obtained according Bax and Subramanian pulse sequence [22]. Spectral widths of 21,381 Hz in ^{13}C and 4505 Hz in ^1H dimensions were used to collect a 4096 × 512 (TPPI) point data matrix with 32 scans/t1 value expanded to 4096 × 1024 by zero filling. The relaxation delay was 1 s. A sine bell window shifted by π/2 was applied in both dimensions. The HMQC-HOHAHA spectrum was obtained using the Lerner and Bax pulse sequence [23]. Spectral widths of 18,865 Hz in ^{13}C and 4505 Hz in ^1H dimensions were used to collect a 4096 × 512 (TPPI) point data matrix with 80 scans/t1 value expanded

to 4096 × 1024 by zero filling. The relaxation delay was 1 s and the mixing time (τ_m) 59 ms. A sine bell window shifted by $\pi/2$ was applied in both dimensions. The HMBC was obtained according Bax and Summers pulse sequence [24]. Spectral widths of 44,019 Hz in ^{13}C and 4505 Hz in ^{1}H dimensions were used to collect a 4096 × 512 (TPPI) point data matrix with 112 scans/t1 value expanded to 4096 × 1024 by zero filling. The relaxation delay was 1 s.

Results

Purification of arabinomannans

The AMs were purified by the previously reported method for extraction and purification of ManLAMs from *M. bovis* BCG cell wall [9]. Two types of AMs were isolated according to their extraction mode and designed as parietal and cellular. This new procedure, using a Triton X-114 phase separation technique, fractionated hydrophilic polysaccharides (AMs) and amphipathic mannoconjugates (ManLAMs and LMs). AMs were further purified by Bio-Gel P-100 gel filtration. In the previous study, the compounds recovered at this step were identified as polysaccharides since they were found in the hydrophilic detergent-depleted phase after the Triton X-114 phase separation and they did not migrate on SDS-PAGE. Using monosaccharide analysis, they were identified as AMs by the presence of mannose and arabinose.

General structural features

The molecular mass of pAMs was investigated by MALDI/MS. The MALDI-TOF mass spectrum of pAMs (Fig. 1) exhibited one intense broad peak centered at *m/z* 16,000 assigned to molecular ions, indicating a molecular mass for the major glyco-forms of 16 kDa. This attribution was confirmed by the presence of two other peaks of lower intensity at *m/z* 33,000 and 49,000 attributed to di- and trimeric forms, respectively.

An overall view of AM structure was obtained by comparing the 1D ^{1}H NMR spectra of the AMs and ManLAMs. Figure 2 shows the 1D ^{1}H spectra of pAMs (a) and cellular ManLAMs (b). These two molecules exhibited very similar anomeric regions (Fig. 2c and d) indicating comparable carbohydrate domain structures for ManLAMs and AMs. However, the resonances at high field (0.9 and 1.3 ppm) in the cellular ManLAM spectrum (Fig. 2b), typifying the presence of fatty acids, were not observed with the pAMs (Fig. 2a) and cAMs (not shown). Moreover, no significant amounts of fatty acids were detected by gas chromatographic analysis after alkaline hydrolysis of pAMs and cAMs. Taken together, these results demonstrated the hydrophilic nature of pAMs and cAMs recovered in the detergent-depleted phase by the Triton X-114 phase separation method.

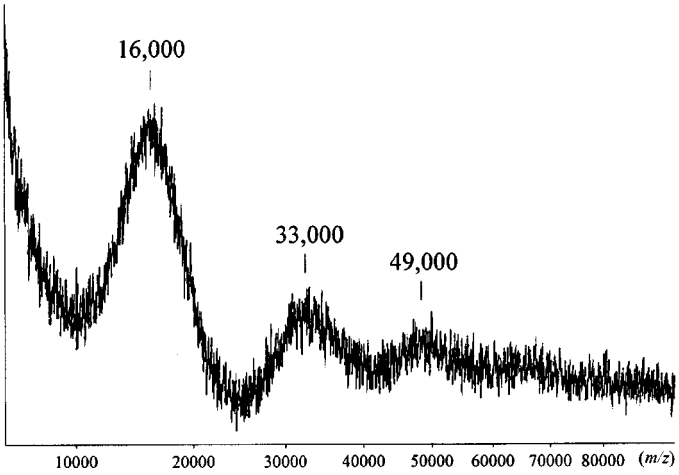

Figure 1. Positive-ion MALDI mass spectrum of pAMs from *M. bovis* BCG in 9:1 mixture of 2,5-dihydroxybenzoic acid with 2-hydroxy-5-methoxybenzoic acid as matrix.

Mannooligosaccharide caps

The presence of mannooligosaccharide caps in pAMs and cAMs was investigated by ^{1}H-^{13}C HMQC experiments (data not shown) as previously described by Venisse *et al.* [15]. The pAM C-1 resonances at δ 104.7 and δ 100.8 were respectively assigned to 2-α-Man*p* and t-α-Man*p* residues. Each of these resonances correlated with two different proton resonances at δ 5.14, δ 5.12 and δ 5.06, δ 5.04, respectively, in agreement with the presence of (1→2)-α-D-mannooligosaccharide caps [15]. Likewise, the presence of mannooligosaccharide caps was established in the cAMs. The presence of these caps was also supported by the identification of 2-Man*p* residues from the methylation analysis of pAMs and cAMs (not shown). Since mannose-capped LAMs have been designated as ManLAMs, the AMs described here corresponded to ManAMs. The structure of the mannooligosaccharide caps was then investigated by capillary electrophoresis (CZE). Both parietal and cellular ManAMs (pManAMs and cManAMs, respectively) were submitted to mild acid hydrolysis (0.1M HCl for 30 min at 110 °C), which preferentially cleaves arabinofuranosyl linkages, and to APTS tagging by reductive amination. Finally, the APTS oligosaccharide derivatives were analyzed by CZE monitored by laser-induced fluorescence [9]. The electrophoregram of the APTS derivatives from the pManAMs (Fig. 3) exhibited several peaks, which were assigned by coelectrophoresis using oligosaccharide-APTS standards and by previous data on ManLAM mannooligosaccharide structures determined by CZE coupled to electrospray ionization mass spectrometry [25]. The different mannooligosaccharide caps were quantified by peak integration [18]. The major structural motif was the dimannosyl unit (75%), while mannosyl (16%) and trimannosyl (9%) were less frequent. CZE analysis of cManAMs re-

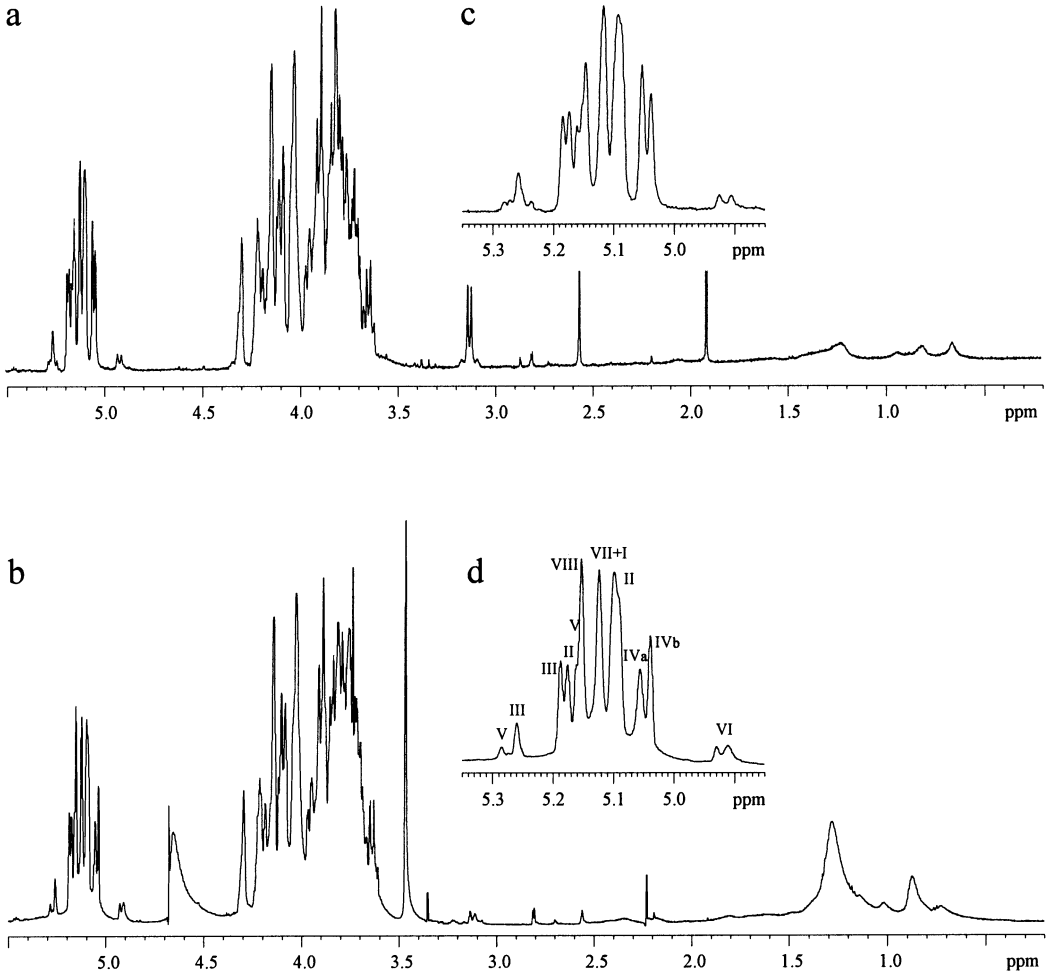

Figure 2. 1D ^{1}H spectra of pAMs (a, c) and cellular ManLAMs (b, d) in D_2O at 313 K. Full spectra (δ ^{1}H: 5.50 - 0.20) (a, b) and anomeric region (δ ^{1}H: 5.35 - 4.85) (c, d) are shown. I, 3,5-α-Ara*f;* II, 5-α-Ara*f;* III, 2-α-Ara*f;* IV, t-α-Man*p;* V, t-β-Ara*f;* VI, 6-α-Man*p;* VII, 2-α-Man*p;* VIII, 2,6-α-Man*p.* These resonances (d) were assigned according ^{1}H-^{13}C HMQC, HMQC-HOHAHA and ^{1}H-^{1}H HOHAHA experiments (not shown).

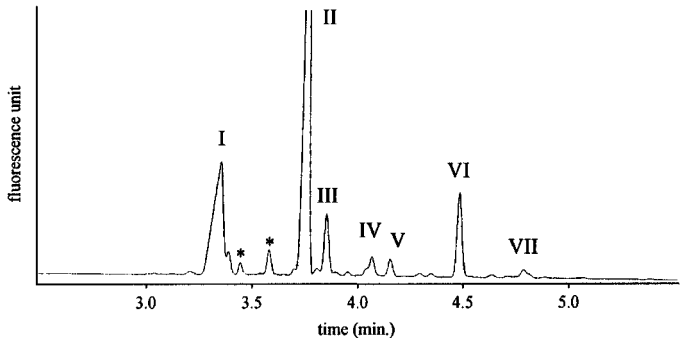

Figure 3. Electrophoregram of oligosaccharide derivatives obtained from pManAMs after mild acidic hydrolysis (0.1M HCl, 30 min at 110 °C) and derivatization with APTS. Analysis was carried out with a 470 mm × 50 μm capillary, at a temperature of 20 °C with an applied voltage of 24 kV and monitored by laser-induced fluorescence. Acetic acid 1% (w/v), triethylamine 30 mM in water pH 3.5 was used as running electrolyte. Peak I, APTS; peak II, Ara-APTS; peak III, Man-APTS; peak IV, Ara*f*-Ara-APTS; peak V, Man*p*-Ara-APTS; peak VI, Man*p*-Man*p*-Ara-APTS: peak VII, Man*p*-Man*p*-Man*p*-Ara-APTS. Peaks labeled with stars (*) arise from the reagent.

vealed the presence of the same mannooligosaccharide cap structures and in similar amounts to pManAMs, dimannosyl (65%), mannosyl (23%) and trimannosyl (12%).

Mannan core

pManAM and cManAM mannan cores were obtained after mild acidic hydrolysis (0.1M HCl for 30 min at 110 °C) and dialysis to separate the mono- and oligosaccharides (those previously analyzed by CZE) from the non-hydrolyzed mannan.

Initially the glycosidic linkages were analyzed qualitatively by methylation (not shown). t-Man*p* and 2,6-Man*p* were the most abundant mannosyl residues of the pManAM and cManAM mannan cores. A low proportion of 6-Man*p* residues was recovered. The absence of 2-Man*p* residues confirmed that these latter were only present in the mannooligosaccharide cap structures. The presence of arabinosyl residues, in low amounts, indicated an incompletely degraded arabinan domain.

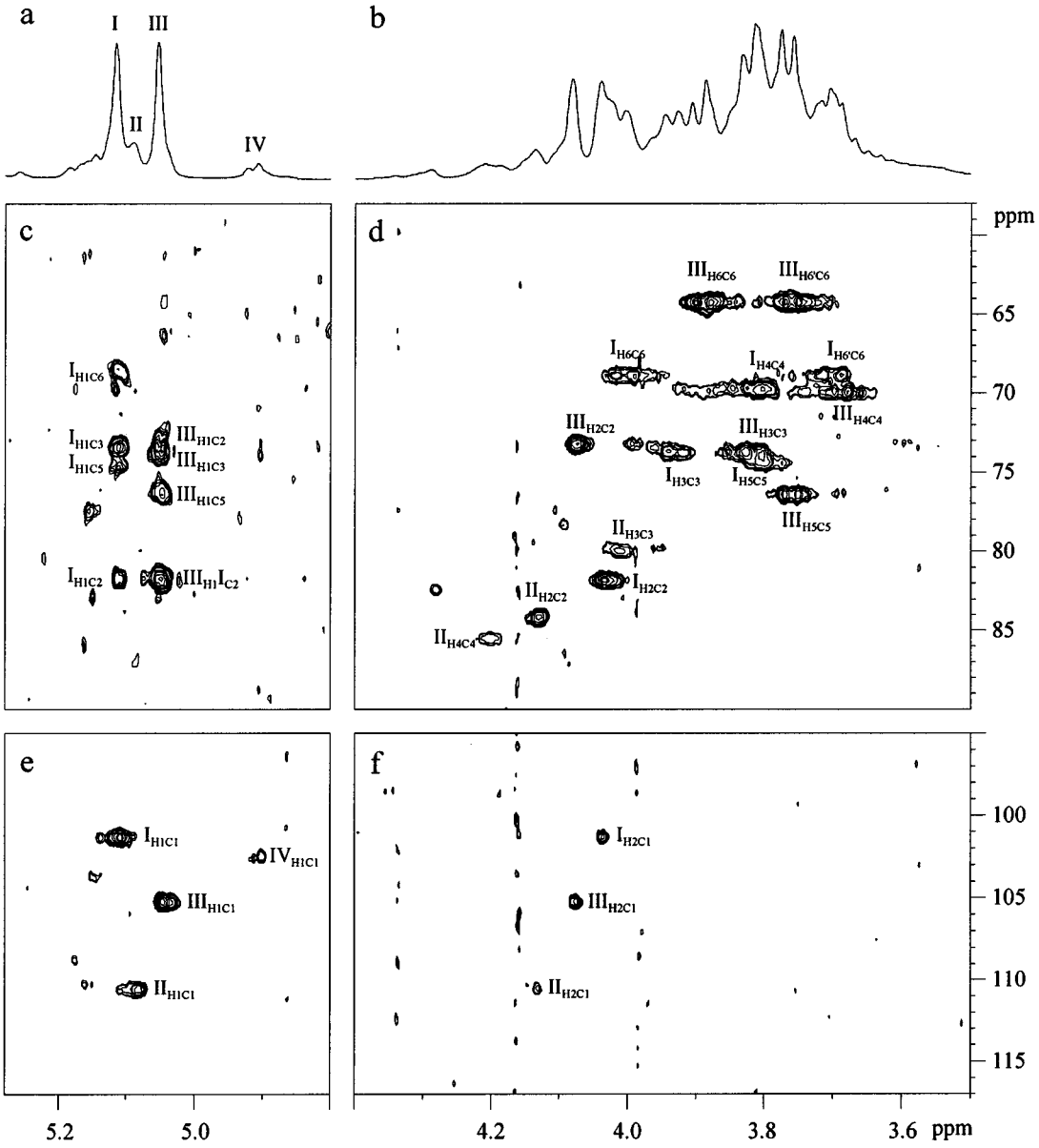

Figure 4. 1D ^{1}H (a, b) and 2D ^{1}H-^{13}C HMBC (c), ^{1}H-^{13}C HMQC (d, e), ^{1}H-^{13}C HMQC-HOHAHA τ_m 59 ms (f) spectra of pManAM mannan core in D_2O at 313 K. Expanded regions (δ ^{1}H: 4.80–5.28) (a), (δ ^{1}H: 3.50–4.40) (b), (δ ^{1}H: 4.80–5.28, δ ^{13}C: 58–90) (c), (δ ^{1}H: 3.50–4.40, δ ^{13}C: 58–90) (d), (δ ^{1}H: 4.80–5.28, δ ^{13}C: 95–117) (e), (δ ^{1}H: 3.50–4.40, δ ^{13}C: 95–117) (f) are shown. Glycosyl residues are labeled in roman numerals and their carbons and protons in Arabic numerals. For example, III_{H2C1} means a correlation between proton H-2 and carbon C-1 of residue III; $III_{H1}I_{C2}$ means a correlation between proton H-1 of residue III and carbon C-2 of residue I. I, 2,6-α-Man*p*; II, 5-α-Ara*f;* III, t-α-Man*p;* IV, 6-α-Man*p.*

A quantitative analysis of the glycosidic linkages was deduced from NMR data. The anomeric proton resonance region of the pManAM mannan core (Fig. 4a) was dominated by two intense signals at δ 5.11 (I) and δ 5.05 (III) and two weaker signals at δ 5.08 (II) and δ 4.90 (IV). Anomeric proton and carbon signals were routinely assigned from the ^{1}H-^{13}C HMQC experiment (Fig. 4e) based on our previous results with LAMs [15,26] and LMs [27]. Resonances I, II, III and IV were assigned to 2,6-α-Man*p,* 5-α-Ara*f,* t-α-Man*p* and 6-α-Man*p,* respectively (Table 1). Determination of the glycosidic linkages required the attribution of the different proton and carbon resonances for each spin system. These resonances were partially attributed from the ^{1}H-^{1}H HOHAHA (not shown), ^{1}H-^{13}C HMQC (Fig. 4d and 4e) and ^{1}H-^{13}C HMQC-HOHAHA (Fig. 4f) experiments. The assignments are summarized in Table 1. Glycosidic linkages were investigated by ^{1}H-^{13}C HMBC experiment (Fig. 4c). H-1 of 2,6-α-Man*p* units (I) at δ 5.11 showed intracyclic correlations with C-2 at δ 81.7, C-3 at δ 73.6, C-5 at δ 74.3. An additional intercyclic connectivity with C-6 at

Table 1. Proton and carbon chemical shifts of mild acidic hydrolyzed pManAMs. Chemical shifts were measured at 313 K in D_2O and are referenced relative to internal acetone at δ_H 2.225 and δ_C 34.00.

	Chemical shifts (ppm)					
Residue	*H-1* *C-1*	*H-2* *C-2*	*H-3* *C-3*	*H-4* *C-4*	*H-5(H-5′)* *C-5*	*H-6/H-6′* *C-6*
I: 2,6-*O*-α-Man*p*	5.11 101.3	4.03 81.7	3.93 73.6	3.80 69.7	3.78 74.3	4.01/3.70 68.9
II: 5-*O*-α-Ara*f*	5.08 110.6	4.13 84.1	4.01 79.8	4.20 85.5	nd	—
III: t-α-Man*p*	5.05 105.2	4.07 73.1	3.81 73.7	3.69 69.9	3.76 76.4	3.89/3.76 64.2
IV: 6-α-Man*p*	4.90 4.91 102.4 102.6	nd	nd	nd	nd	nd

nd = not determined

δ 68.9 indicated that 2,6-α-Man*p* units were interconnected by (α1 →6) glycosidic linkages. H-1 of t-α-Man*p* units (III) at δ 5.05 correlated with their C-2 at δ 73.1, C-3 at δ 73.7, C-5 at δ 76.4. A connectivity with C-2 of 2,6-α-Man*p* units at δ 81.7 established that 2,6-α-Man*p* were substituted at O-2 by t-α-Man*p* residues. This was confirmed by the presence of a correlation between C-1 of t-α-Man*p* at δ 105.2 and H-2 of 2,6-α-Man*p* at δ 4.03 (not shown). Taken together, these data demonstrate that the mannan core of pManAMs is a multibranched structure composed by (α1→6) Man*p* backbone substituted at O-2 by t-α-Man*p* units. As previously established by the methylation data (not shown), the NMR study confirmed that the mannan core contained a low proportion of 6-α-Man*p*. Indeed, a ratio 2,6-α-Man*p*:t-α-Man*p*:6-α-Man*p*, 11:10:2 was obtained by integration of the anomeric proton signals, confirming a highly branched structure and providing a branching degree (2,6-α-Man*p*/ (2,6-α-Man*p* + 6-α-Man*p*) ratio) of 84%. The integration of the anomeric proton signals on the 1D ^1H spectrum of cManAM mannan core provided the same value (84%) for the mannan core branching degree.

Reducing end

In order to determine if ManAMs possessed a reducing end, ManAMs were submitted to ANDS tagging followed by reductive amination. The mixture was then subjected to SDS-PAGE. The gel was revealed under a UV lamp at 254 nm (Fig. 5). The fractions containing pManAMs (lanes b and c) showed a fluorescent band. As expected, the ManLAM fraction (lane d) was not revealed. Moreover, the fractions containing free ANDS (lane a) or pManAMs plus ANDS, but not submitted to the tagging reaction (lane e) were not revealed, indicating that in lanes b and c, ANDS was covalently attached to pManAMs. Taken together these results indicated that pManAMs possessed a reducing end. Using a similar approach, the pManAM and cManAM mannan cores were shown to be tagged by ANDS, demonstrating the presence of a ManAM reducing end on the mannan core. We further quantified the degree of ManAM labeling by ANDS. Different amounts of

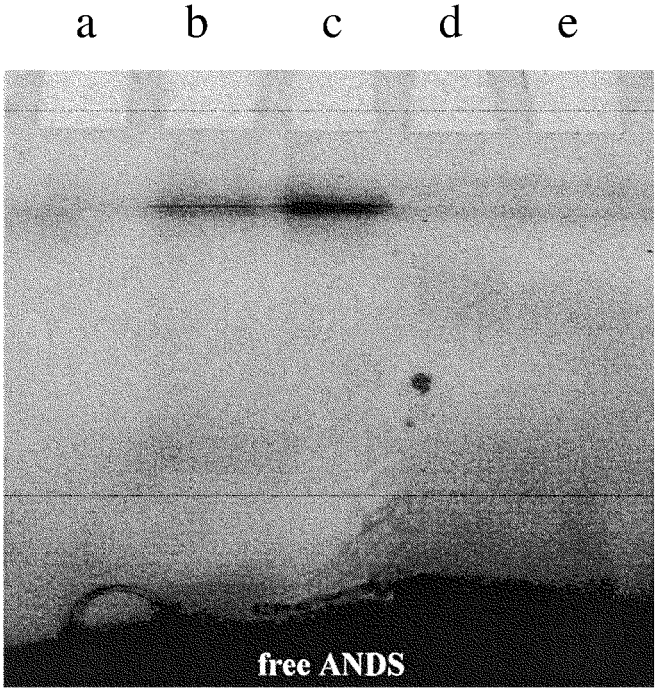

Figure 5. Negative photograph of a PAGE electrophoretogram of ANDS-derivatized ManAMs and ManLAMs, from *M. bovis* BCG, revealed under UV light. Free ANDS (lane a), 50 μg pManAMs ANDS-derivatized (lane b), 100 μg pManAMs ANDS-derivatized (lane c), 200 μg ManLAMs ANDS-derivatized (lane d), 200 μg pManAMs + ANDS non-derivatized (lane e).

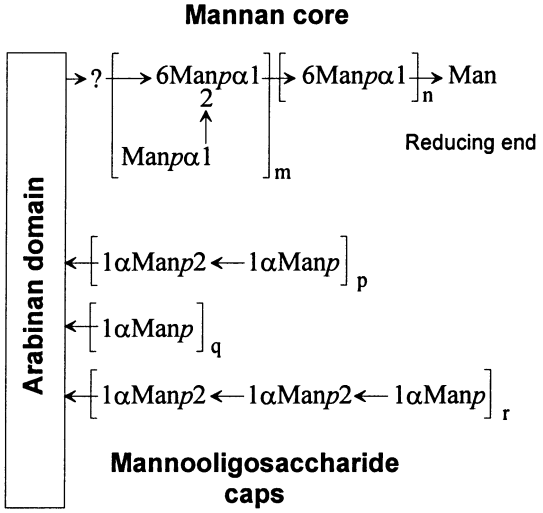

Figure 6. Schematic representation of ManAMs from *Mycobacterium bovis* BCG. Mannan core and mannooligosaccharide caps are detailed. The value of 84% for the mannan core branching degree indicates a ratio m/n of 5.25. CZE analysis of mannooligosaccharide caps gives the ratios p/q of 4.69 and p/r of 8.33 for pManAMs and p/q of 2.83 and p/r of 5.41 for cManAMs. Arabinan domain consists predominantly of a →5-α-D-Ara*f*-1→ backbone punctuated by branching produced by 3,5-α-D-Ara*f* residues.

ManAMs (from 0 to 500 μg) were submitted to ANDS tagging. After the tagging reaction, excess ANDS was removed by electrodialysis. Using an ANDS calibration curve established at 254 nm, we found that only 37 ± 3% ManAMs were labeled by ANDS. In this respect, it has been demonstrated that the effectiveness of fluorescent labeling decreases with increasing molecular mass of the polysaccharide [28]. Indeed, using a dextran with average molecular mass of 18,300, Chmelik *et al.* [28], by comparison of size-exclusion and CZE data, estimated that only 30–50% of the original dextran was labeled with aminonaphthalene trisulfonate (ANTS). We assumed therefore that nearly all the ManAM molecules possessed a reducing end.

Discussion

AMs isolated from different mycobacteria have been abundantly described (for a review, see [29]). They are mainly found as exocellular [30] or surface-exposed [31] polysaccharides. The AMs from *M. bovis* BCG studied here were isolated from two independent fractions, the parietal one obtained from ethanol/water extracts of delipidated mycobacteria and the cellular one obtained after disintegration of the resulting bacteria [9]. Despite delipidation by chloroform/methanol extractions, which probably drastically disturbs the ultrastructure of mycobacteria, the existence of "cellular" AMs suggested the presence of an AM pool embedded in the mycobacterial envelope. We have also found evidence for an AM pool in the cellular fraction of *M. tuberculosis* H37Rv (Gilleron M, Bala L, Brando T, Vercellone A, and Puzo G, unpublished results).

From a structural point of view, AMs were isolated in the detergent-depleted phase, i.e. hydrophilic phase, during the Triton X-114 phase separation method, establishing their hydrophilic nature. These data were in agreement with the gas chromatographic and NMR data which revealed the absence of fatty acids.

The molecular mass of pManAMs as determined by MALDI/MS was found to be 16 +/− 3 kDa. This value is similar than that found for ManLAMs, 17 +/− 5 kDa [15]. In common with ManLAMs, ManAMs exhibited a marked dispersion in molecular mass attributed to different glycoforms. The value of 16 kDa, determined by MALDI/MS, resembled those found, by indirect methods, for the previously described AMs: i) 10 kDa for *M. tuberculosis* Aoyama B AMs as determined by ultracentrifugal analyses [32], ii) 13 kDa for AMs from different mycobacterial strains determined by Lemassu *et al.* [30,33] and Ortalo-Magné *et al.* [31] by gel permeation, iii) 14 kDa for *M. paratuberculosis* lipid-free AMs, also determined by gel permeation [34].

The present structural study of AMs was focused on two domains, the mannooligosaccharide caps and the mannan core.

AMs, in common with ManLAMs from *M. bovis* BCG, were found to be capped by mannooligosaccharide units. The structure of these caps, determined by capillary electrophoresis, was the same as that previously described for ManLAMs [9,25]. As observed for ManLAMs, the dimannosyl unit was the most abundant motif, while the mannosyl and trimannosyl units were less frequent. In order to determine the capping extension, one can calculate the "capping degree" which corresponds to the ratio between the number of arabinan side chains terminated by Man*p* units and the total number of arabinan side chains [35]. This value is determined from the methylation analysis by the ratio (3,5-di-*O*-linked-Ara*f*-t-Ara*f*) to 3,5-di-*O*-linked-Ara*f*. A capping percentage of 50 and 60% was found for pManAMs and cManAMs, respectively. Nevertheless, as previously noted by others [31] and us [3], the relative abundance of alditol acetates recovered after methylation does not accurately reflect the relative abundance of the corresponding monosaccharides composing ManLAMs and ManAMs. The capping percentages determined by this method may need to be revised, and accurate values for the capping percentage of ManAMs and ManLAMs will have to await development of another method for determining the relative abundance of the different monosaccharides.

The mannan core was found to be highly branched as a branching degree of 84% was established for both pManAMs and cManAMs. The branching degree resembled that found for the mannan region of the non-phosphorylated LAMs (75%) described by Venisse *et al.* [26], which

corresponds in fact to the pManAMs described in the present study. It is also noteworthy that the branching degree of the mannan core of *M. bovis* BCG ManAMs was slightly higher than that of the *M. bovis* BCG ManLAMs (67%) [26] and different *M. tuberculosis* ManAMs, which ranged from 52% to 79% [31].

We showed that these ManAMs possessed a reducing end localized on the mannan core, and consequently lacked the PI anchor present in ManLAMs.

Taken together these data demonstrate that the structure of pManAMs and cManAMs closely resembles that of ManLAMs (Fig. 6). No substantial differences were observed either in the mannooligosaccharide caps since the same motifs were present in similar amounts, or in the mannan cores, which are highly branched in both ManAMs and ManLAMs. The main difference was the absence of the PI anchor in ManAM molecules. These results indicate the important role of the PI anchor in the biological properties of ManLAMs.

Acknowledgments

This work was supported by grants from the Région Midi-Pyrénées (RECH/9407528), from the Mission Scientifique et Technique du Ministère de l'Education Nationale, de l'Enseignement Supérieur et de la Recherche (ACC SV6 N 9506005). We thank Thermo Bioanalysis for the recording of ManAM MALDI-TOF spectra.

References

1 Collins FM (1998) *Front Biosci* **3:** e123–32.
2 Chatterjee D, Khoo KH (1998) *Glycobiology* **8:** 113–20.
3 Vercellone A, Nigou J, Puzo G (1998) *Front Biosci* **3:** e149–63.
4 Barnes PF, Chatterjee D, Abrams JS, Lu S, Wang E, Yamamura M, Brennan PJ, Modlin RL (1992) *J Immunol* **149:** 541–7.
5 Zhang Y, Broser M, Cohen H, Bodkin M, Law K, Reibman J, Rom WN (1995) *J Clin Invest* **95:** 586–92.
6 Gilleron M, Himoudi N, Adam O, Constant P, Venisse A, Rivière M, Puzo G (1997) *J Biol Chem* **272:** 117–24.
7 Yoshida A, Koide Y (1997) *Infect Immun* **65:** 1953–5.
8 Riedel DD, Kaufmann SH (1997) *Infect Immun* **65:** 4620–3.
9 Nigou J, Gilleron M, Cahuzac B, Bounery JD, Herold M, Thurnher M, Puzo G (1997) *J Biol Chem* **272:** 23094–103.
10 Schlesinger LS, Hull SR, Kaufman TM (1994) *J Immunol* **152:** 4070–9.
11 Venisse A, Fournie JJ, Puzo G (1995) *Eur J Biochem* **231:** 440–7.
12 Sieling PA, Chatterjee D, Porcelli SA, Prigozy TI, Mazzaccaro RJ, Soriano T, Bloom BR, Brenner MB, Kronenberg M, Brennan PJ, Modlin RL (1995) *Science* **269:** 227–30.
13 Delmas C, Gilleron M, Brando T, Vercellone A, Gheorghui M, Rivière M, Puzo G (1997) *Glycobiology* **7:** 811–7.
14 Nigou J, Gilleron M, Puzo G (1999) *Biochem J* **337:** 453–60.
15 Venisse A, Berjeaud JM, Chaurand P, Gilleron M, Puzo G (1993) *J Biol Chem* **268:** 12401–11.
16 Tsarbopoulos A, Karas M, Strupat K, Pramanik BN, Nagabhushan TL, Hillenkamp F (1994) *Anal Chem* **66:** 2062–70.
17 Jackson P (1990) *Biochem J* **270:** 705–13.
18 Guttman A, Chen FT, Evangelista RA, Cooke N (1996) *Anal Biochem* **233:** 234–42.
19 O'Shea MG, Morell MK (1996) *Electrophoresis* **17:** 681–8.
20 Marion D, Wüthrich K (1983) *Biochem Biophys Res Commun* **113:** 967–74.
21 Shaka AJ, Barker PB, Freeman R (1985) *J Magn Reson* **64:** 547–52.
22 Bax A, Subramanian S (1986) *J Magn Reson* **67:** 565–9.
23 Lerner L, Bax A (1986) *J Magn Reson* **69:** 375–80.
24 Bax A, Summers MF (1986) *J Am Chem Soc* **108:** 2093–4.
25 Monsarrat B, Brando T, Condouret P, Nigou J, Puzo G (1999) *Glycobiology* **9:** 335–42.
26 Venisse A, Riviere M, Vercauteren J, Puzo G (1995) *J Biol Chem* **270:** 15012–21.
27 Gilleron M, Nigou J, Cahuzac B, Puzo G (1999) *J Mol Biol* **285:** 2147–60.
28 Chmelik J, Chmelikova J, Novotny MV (1997) *J Chromatogr A* **790:** 93–100.
29 Daffé M, Draper P (1998) *Adv Microb Physiol* **39:** 131–203.
30 Lemassu A, Daffé M (1994) *Biochem J* **297:** 351–7.
31 Ortalo-Magné A, Andersen AB, Daffé M (1996) *Microbiology* **142:** 927–35.
32 Misaki A, Azuma I, Yamamura Y (1977) *J Biochem (Tokyo)* **82:** 1759–70.
33 Lemassu A, Ortalo-Magné A, Bardou F, Silve G, Laneelle MA, Daffé M (1996) *Microbiology* **142:** 1513–20.
34 Sugden EA, Samagh BS, Bundle DR, Duncan JR (1987) *Infect Immun* **55:** 762–70.
35 Chatterjee D, Lowell K, Rivoire B, McNeil MR, Brennan PJ (1992) *J Biol Chem* **267:** 6234–9.

Received 12 February 1999, revised 11 May 1999, accepted 11 May 1999